Pergamon

Geochimica et Cosmochimica Acta, Vol. 61, No. 13, pp. 2679–2690, 1997

0016-7037/97 $17.00 + .00

PII S0016-7037(97)00101-4

Lithium isotope composition of Quaternary and Tertiary biogene carbonates and a global lithium isotope balance

JOCHEN HOEFS and MICHAEL SYWALL
Geochemisches Institut der Universität, Goldschmidstrasse 1, D-37077 Göttingen, Germany

(*Received June* 21, 1996; *accepted in revised form February* 28, 1997)

Abstract—The lithium isotope composition of thirty-nine foraminifera samples and twenty-one carbonate oozes from the Atlantic and the Indian oceans (0 to 81 Ma) has been determined by thermionic mass spectrometry. Using ocean water as external standard, Lithium isotope variations of about 40‰ have been observed.

Holocene foraminifera samples possess a well-defined mean lithium isotope composition of +13‰ relative to ocean water, whereas Tertiary foraminifera show a total variation range from −10 to +30‰. This variability of the lithium isotope signature may be interpreted as reflecting shifts in the paleo-ocean water composition, although the influence of diagenetic effects cannot totally be excluded. In a steady-state system variations of the lithium input to the ocean cannot cause shifts in the δ^6Li of ocean water exceeding 15‰. To match the mean variation range observed in foraminifera, a nonsteady-state ocean has to be assumed and that the input fluxes varied by about a factor of 2 throughout time. *Copyright © 1997 Elsevier Science Ltd*

1. INTRODUCTION

The study of geochemical cycles is an important tool for understanding processes of global change. In this context the element lithium is a promising, yet an almost neglected geochemical parameter. Lithium is of moderate mantle incompatibility (Ryan and Langmuir, 1987) and, because of its relatively small ion (r_{Li^+} = 0.59 Å), it is able to substitute for Mg^{2+} in crystal-lattices (Heier and Billings, 1970). In addition its high ion-potential induces a very strong hydration of the lithium ion in aqueous systems. Thus, lithium shows a unique geochemical behaviour in comparison to the other alkali homologues. The discovery of the important lithium input to the ocean via the mid-ocean-ridge (MOR) hydrothermal systems (Edmond et al., 1979) provided great progress in the investigation of the exogene lithium cycle. However, the global lithium mass balance is still poorly defined:

Lithium is supplied to the ocean mainly from two sources: By high-temperature(=HT) basalt-ocean-water reactions and as river input from the weathering of continental crust. In hydrothermal systems near the mid-ocean-ridges, lithium is leached from oceanic basalts at temperatures >250°C. Lithium concentrations of the escaping hydrothermal solutions vary between 4 and 9 ppm (Ø = 7 ppm) (von Damm et al., 1985a,b). Because of retrograde metamorphic reactions near the vent-orifice lithium is not completely leached from basalt. Calculations of the lithium HT-input by Stoffyn-Egli and Mackenzie (1984), Ryan and Langmuir (1987), and Chan et al. (1994) suggest flux rates between 10 and 20×10^{10} gLi/a. A mean global lithium concentration of river water of Ø = 3 ppb has been calculated from a broad database by Edmond et al. (1979). This leads to an estimate of lithium input by continental run-off in the order of 9 to 11×10^{10} gLi/a. Thus, calculation of a lithium mass balance assuming steady state produces a surplus of lithium in the order of 19×10^{10} gLi/a to 31×10^{10} gLi/a. To remove this excess lithium from the ocean water system, the following processes must be taken into account.

1.1. Low Temperature (LT)-Alteration of Oceanic Crust

Below temperatures of about 250°C the oceanic crust is altered by reactions with ocean water, a process which is commonly termed "spilitisation" and which implies the uptake of lithium in the basalts (Thompson, 1983). Estimates of LT-lithium output range from 3×10^{10}g Li/a to 13×10^{10} g Li/a. (Mengel and Hoefs, 1990; Seyfried et al., 1984; Stoffyn-Egli and Mackenzie, 1984).

1.2. Biogene Carbonate Production

Marine carbonates contain 2 ppm lithium on average. Assuming an accumulation rate in the order of 1.1×10^{15}g $CaCO_3$/a (Milliman, 1974) to 3×10^{15}g $CaCO_3$/a (Morse and Mackenzie, 1990), lithium amounts between 0.2 $\times 10^{10}$g Li/a and 0.6 $\times 10^{10}$g Li/a can be extracted from the ocean reservoir.

1.3. Biogene Opal and Chert Production

Ishikawa and Nakamura (1993) determined a mean lithium content of 30 ppm for Quaternary radiolarian and 31 ppm for diatomaceous oozes. Maxwell (1963) reported lithium concentrations in cherts between 2 and 36 ppm (Ø = 11 ppm). With a global accumulation rate of 7×10^{14}g SiO_2/a (Calvert, 1974) biogene opal production could be responsible for the output of 2×10^{10}g Li/a.

1.4. Diagenesis of Clay-Minerals and Authigenic Clay-Mineral Production

This has been postulated as the most important sink for lithium in the ocean (Chan et al., 1992; Stoffyn-Egli and

Mackenzie, 1984; Seyfried et al., 1984). Seyfried et al. (1984) included nearshore sediments in their calculations and estimated a value of 19.4×10^{10}g Li/a as possible output-flux. This flux may be overestimated, because near shore sediments are not in equilibrium with open ocean water. We consider a lower value of 5×10^{10} g/a Li to be a better approximation for the ocean. Table 1 summarizes the most important lithium sinks and sources. The large range of +10.7 to −6.3 indicates a lack of information of the contributions of the sinks and sources; in particular for the sinks "clay mineral diagenesis" and "low-temperature alteration."

As we will show in this study the analysis of lithium isotope ratios allows new insights into the global lithium cycle. The element lithium has two stable isotopes with the masses 6 and 7. Until the mid-eighties little informations were available about variations of the lithium isotope composition and related fractionation effects. Since then mainly through the efforts of Chan (1987), Chan and Edmond (1988), Chan et al. (1992), Chan et al. (1993), Chan et al. (1994), and You et al. (1995) major advances in the isotope geochemistry of lithium have been achieved.

The determination of lithium isotope ratios by thermal ionisation mass spectrometry suffers from technical analytical difficulties: (1) during evaporation and ionization of lithium, thermal isotope fractionations occur in the ion source, due to the high relative mass difference of 16.7% between the two lithium isotopes. This effect may cause a decrease of the $^6Li/^7Li$-ratio during the measurement. (2) The formation of lithium compounds with different volatility and/or ionization-energy causes a "reversed," "enhanced," or an apparently "zero"-fractionation (Habfast, 1983). These processes result in increasing $^6Li/^7Li$ ratios, very steeply decreasing $^6Li/^7Li$ ratios or constant but biased $^6Li/^7Li$ ratios, respectively. (3) Furthermore, TIMS measurements require the separation of lithium from the sample matrix. If no precautions are taken, cation-exchange-processes may lead to measurable fractionation effects already on the exchange column.

Green et al. (1988), Chan (1987), and Datta et al. (1992) tried to minimize these problems by measuring chemical compounds of lithium instead of analysing the masses 6 and 7 directly. The relative mass difference of Lithium compounds decreases with increasing molecular weight of the compounds. This in turn should lead to smaller isotope fractionations with growing mass number of the chemical compound. However, a disadvantage of this method is the higher amount of lithium required to obtain a sufficient ion intensity (between 1 to 4 μg). To overcome these problems we developed a method analysing masses 6 and 7 directly to determine amounts of 10 to 100 ng lithium. The general impetus of this work is based on the studies of Svec and Anderson (1965), Flesch and Svec (1973), Brown et al. (1977), Michiels and deBiévre (1983), Boerboom (1989), and Xiao and Beary (1989). A similar method analysing ^7Li and ^6Li has recently been described by You and Chan (1996).

Table 1. Global lithium mass balance.

Source and sinks	Range (10^{10}gLi/a)
HT-alteration of oceanic crust	+10 to +20
Continental run-off, river-input	+9 to +11
LT-alteration of oceanic crust	−3 to −14
Clay-mineral-diagenesis	−5 to −19
Carbonate-production	−0.2 to −1.8
Opal-production	−0.1 to −2.5
	+10.7 to −6.3

In this paper we present a comprehensive study of lithium isotope ratios in Holocene to Tertiary planktonic foraminifera and Tertiary carbonate oozes, which contain lithium in the concentration range between 0.2 to 4 ppm. We will argue that the lithium isotope ratios observed in fossil biogene carbonates can be interpreted as tracers of the paleo-ocean water composition. In addition, a few Phanerozoic carbonate rocks and recent marine bivalvia shells have been analyzed.

2. ANALYTICAL TECHNIQUES

2.1. Chemical Preparation

Samples from DSDP and ODP drill cores, which were provided by courtesy of W. U. Ehrmann, A. Mackensen, N. Scheele (Alfred-Wegener-Institut. Bremerhaven, FRG), and H. Oberhänsli (Max-Planck-Institut Mainz, FRG), were suspended in distilled water and the >125 μm fraction was separated by wet sieving. The foraminifera-enriched fraction was inspected under the stereomicroscope and benthic foraminifera, sceletal parts of other organisms, and impurities were removed by handpicking. Bivalvia shells and carbonate rocks were crushed in an agate mortar. The carbonate oozes selected for bulk analysis were freeze-dried and crushed. In a following step all samples were ultrasonically cleaned for 1 min and washed several times with double-distilled water and acetone. The subsequent chemical preparation procedure was performed under clean-room conditions to avoid contaminations. 20 to 100 mg sample material was mixed with 6 mL distilled 1 N HNO_3 in Teflon beakers for 3 hr. Any insoluble silicate or organic residues were separated by centrifuging. The supernate was eventually decanted and transferred into polyethylene-bottles preconditioned with distilled 1 N HNO_3. Subsequently the lithium fraction in the aqueous solution was separated from the carbonate matrix by a two-step cation-exchange procedure using DOWEX 50W-X8 resin as stationary phase and nitric acid as eluent. The columns are made of ultraclean quartz glass. In a first step lithium was separated from the calcium matrix (column efficiency is 90%) and in a second step the resulting lithium fraction was separated (efficiency ≈ 100%) from sodium achieving a yield of 80% and a Na/Li-ratio in the eluate <0.1. A high degree of purity is required, because excess sodium or potassium may cause an instable ion current and higher $^6Li/^7Li$ ratios. This was demonstrated by mixing a lithium-standard with different amounts of sodium and potassium. As shown in Fig. 1, Na/Li- and K/Li-ratios >1 cause a significant increase in the $^6Li/^7Li$-ratio. Cation-exchange processes may be accompanied by fractionation of lithium isotopes: Experiments with sodium zeolites as stationary phase and distilled water as eluent yield a lithium isotope fractionation of 22‰ with ^6Li being more effectively retained than ^7Li (Taylor and Urey, 1938). In order to avoid this fractionation effect a highly acidic eluent (1 N HNO_3) was chosen and a high flow-rate adjusted. Although this induces a relatively poor selectivity for the alkali-elements, it prevents lithium from artificial fractionation. Verification performed with an isotopically well defined synthetic lithium standard (IRM016), revealed no significant shifts in the lithium isotope ratio.

In order to determine the detection limit and to optimize the lithium loading on the filament, experiments were carried out with lithium amounts being stepwisely reduced from 120 ng to 0.5 ng Li. Four samples with a well-defined lithium isotope composition were used. Their $^6Li/^7Li$ ratios remained constant within the 2σ reproducibility until a sample quantity of 10 ng (Fig. 2). Therefore, 50 ng Li must be regarded as optimal filament loading. Since biogene

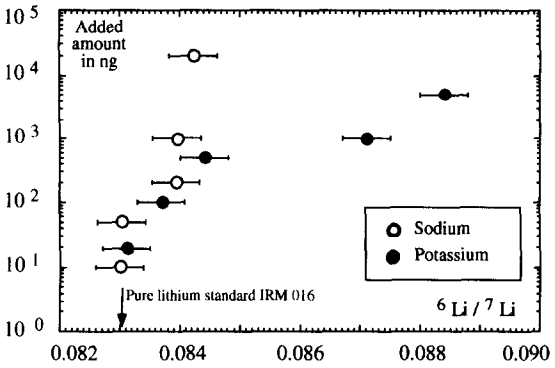

Fig. 1. Influence of admixed sodium and potassium impurities upon the $^6Li/^7Li$-ratio of the lithum standard IRM016. All samples contain a constant amount of 100 ng Li.

carbonates contain 1 ppm lithium on average, about 50 mg of foraminifera are required for a single analysis.

To remove any contaminants both rhenium filaments are heated at the beginning under vacuum with 4.5 ampere for 20 min. For each analysis, an equivalent of 10 to 100 ng lithium were mixed with 2 μg boric acid and loaded on rhenium filaments. This is equivalent to a B/Li-ratio of 20 to 200. The samples were dried upon the filament with an electric current of 1 ampere and afterwards heated for 1 second with 1.8 ampere until a colourless hygroscopic lithium-borate-glass is generated. In order to avoid excessive H_2O-uptake from air, samples were brought into the mass-spectrometer not later than 15 min after loading.

2.2. Mass Spectrometric Procedures

A Finnigan thermal quadrupol-massfilter-system (THQ) working in double-filament technique was used to perform our analysis. Evaporation was carried out by heating the ionization filament, which is arranged parallel to the evaporation filament carrying the sample. To improve the resolution for light masses, the originally installed high-frequency generator was replaced by a sender with better selectivity in the range of the lower mass scale. In order to guarantee maximal reproducibility and to minimize fractionation processes all instrumental parameters were held under nearly constant conditions. Especially the heating procedure and the stability of the ion-current intensity required sensitive control. Based on a large number of measurements a characteristic pattern for the ion current during the heating phase had to be met. Samples which deviated from this pattern were rejected. First signals were received at the secondary electron multiplier at about 1100°C. After a distinct increase of the ion current at the beginning, a phase of decreasing signal-intensity occurred (T = 1250°C ± 30°C) for about 30 min. When the ion current stabilised again, the ionisation filament was further heated to 1350°C ± 25°C. After 1 hr most samples reached a more or less stable signal intensity providing optimal measurement conditions without detectable fractionation. A faraday-cup operating in peak-jumping mode was used as detector. Every single analysis lasted 30 min at least and consisted of ten blocks with six scans per block. After every block, for background correction the signal intensity was measured at mass number 8.5.

The mass spectrometer was calibrated with two lithium compounds with well documented and certified lithium-isotope ratios. The IRM016, standard, a synthetic Li-carbonate with a $^6Li/^7Li$ ratio of 0.08137 (Michiels and deBiévre, 1983) was used for more than two years as external standard. In more than 100 measurements, a ratio of 0.08303 ± 0.00026 has been determined. The other standard is L-SVEC, a NBS standard, which was introduced by Flesch and Svec (1973) with a $^6Li/^7Li$ ratio of 0.0832. For this standard we determined a mean value of 0.08440 ± 0.0004. In both cases the quadrupol-system of the THQ produces a bias in the measured lithium isotope ratios, which has to be corrected for by external standardisation. The instrumental bias was confirmed in a crosscheck, with a thermal magnet-sector mass-spectrometer (MAT 262) at the Finnigan-laboratories in Bremen, where a number of standard and sample measurements showed a systematic offset by about 0.0014.

This observation required an external standardisation. For normalization procedure we utilized ocean water from the Sea of Japan, sampled during ODP Leg 127 (provided by courtesy of H.-J. Brumsack, University of Oldenburg). The results are presented in the conventional δ-notation as δ^6Li, with modern ocean water as external standard:

$$\delta^6 Li^{Sample}_{Ocean\ Water} = \left(\frac{^6Li/^7Li_{Sample}}{^6Li/^7Li_{Ocean\ Water}} - 1\right) \cdot 1000 \qquad (1)$$

By convention, the more abundant isotope ^{7}Li is put in the denominator. Accordingly, negative δ-values denote a "heavy" isotope composition whereas positive δ-values represent a "light" isotope composition. Such a relationship is in opposite to other isotope systematics applied in stable isotope geochemistry.

Chan (1987), Chan and Edmond (1988), Chan et al. (1992, 1993, 1994), You and Chan (1996), and You et al. (1995) standardised their samples against L-SVEC. This standard was also determined in this study, making a comparison of the results for ocean water, basalts, and some marine sediments possible. Figure 5 demonstrates that both datasets are in global agreement with each other showing that both methods of lithium isotope analysis produce comparable results within the limits of precision.

All measured samples are duplicates. Internal precisions of the measurements are generally below 1‰, external precisions including chemical preparation and mass spectrometric measurements are generally not better than 5‰. For multiple measurements ($n \gg 10$) a lower mean standard-deviation of 3‰ was achieved. Considering a natural lithium isotope variation of about 50‰, the technique applied provides significant informations about naturally occurring lithium isotope variations.

Synthetic lithium-tetraborate (Merck), which is used for the production of X-ray fluorescence melt tablets, has a δ^6Li-value of +28‰ well within the range of natural lithium isotope variations. Thus, a contamination even in the range of a few nanograms cannot have caused any detectable shift in δ^6Li. The laboratory blank was determined to be 50 ± 20 pg by isotope-dilution using THQ and by ICP-MS.

2.3. Trace Element Analysis

The lithium concentration of the samples investigated was determined by ICP-MS (VG Plasmaquad) measurements. After

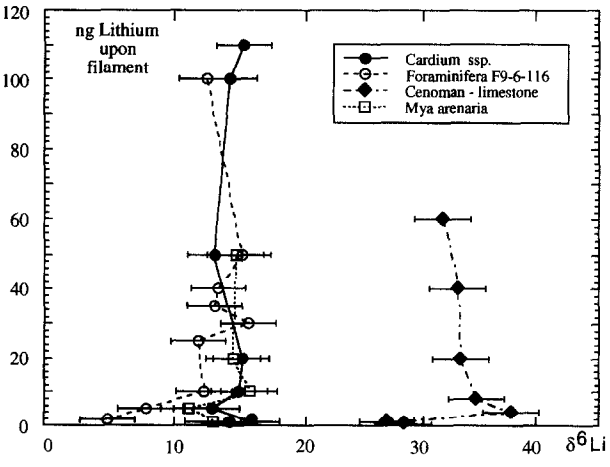

Fig. 2. $^6Li/^7Li$ as a function of the lithium amount on the evaporation filament. Lithium separated from four different carbonates (*Mya ssp.*, *Cardium ssp.*, Cenoman-limestone, foraminifera sample F9-6-116) were loaded in different quantities on the filament.

dissolution of the carbonates with nitric acid a TDS (total dissolved solids) of 8000 ppm was adjusted in the sample solutions. A signal-drift correction was applied by addition of 20 ppb rhodium as internal standard (Stroh and Völlkopf, 1993). Internal laboratory standards were used to reveal systematic bias. The detection limit was 0.2 ppb and the mean relative standard deviation 7%. The best reproducibility was achieved by adjusting the following parameters: Cool-argon: 13.5 L/min, nebulizer flow: 0.93 L/min, auxiliary flow: 1 L/min, sample acquisition time: 60 s, dwell time: 300 μs, data acquisition in peak jump mode, 3 channels/amu. A V-Groove sprayer/atomizer was applied. The mean sensitivity was typically 3×10^4/ppb. The elements Rb, Al, B, and Mn were determined by ICP-MS. Sodium and potassium were analysed separately by AES (Philips PU 9200X), Mg and Sr by ICP-AES (ARL 35000C). $\delta^{13}C$ and $\delta^{18}O$ analyses were performed on a MAT 251 gas-mass-spectrometer. The sample preparation was carried out according to the procedure developed by McCrea (1950).

3. SAMPLES

In order to calibrate the preparation and measurement procedure we measured sample materials being available in sufficient quantities. Therefore, the lithium isotope composition extracted from several bivalvia species (*Abra ssp., Barnea candida, Cardium ssp., Ensis ensis, Macoma baltica, Mya arenaria,* and *Mytilus edulis*), sampled in the litoral of the North Sea (Germany and The Netherlands), were analysed.

Because of the small lithium content of foraminifera at least 50 mg of sample material for one measurement was required. This corresponds to 100 to 1000 individuals depending on their individual size. For this reason the analysis of monospecific or monogeneric foraminifera was not possible and mixed samples had to be used consisting mainly of *globigerina, globorotalia,* and *globoquadrina.* Thirty-nine foraminifera samples were analysed covering a time-span of 57Ma according to the timescale of Harland et al. (1989). The error of the stratigraphic age estimate is generally in the order of ±1Ma. Table 2 summarizes the DSDP and ODP cores, which have been sampled. Additionally one late Pleistocene foraminifera sand from the equatorial Atlantic (RV *Meteor* 9, 1100-4) and five Holocene foraminifera samples from Walfish-Ridge (20°1′S, 8°58′E, RV *Polarstern* PS 2110-1) have been included in the sampling list.

In order to test the suitability of bulk sediments, carbonate oozes from ODP Sites 744 and 738 were analysed as well. These oozes had a mean lithium content of 1.5 ppm and consisted on average of 95% $CaCO_3$. Twenty-one samples covering a timespan from 0.5 to 81Ma were included in the analysis (Table 2).

To study the influence of carbonate diagenesis upon lithium content and lithium isotope composition on biogene marine carbonates, five limestones ranging in age from Cretaceous to Devonian have been analysed as well. Three representative mixtures of German limestones from the Cretaceous, the Jurassic, and the Devonian could be used to obtain mean lithium isotope ratios for these time periods.

Table 2. DSDP and ODP cores which have been sampled for foraminifera by courtesy of H. Oberhänsli (Max-Planck-Institut, Mainz, FRG) and for carbonate oozes by courtesy of W. U. Ehrmann (Alfred-Wegener-Institut, Bremerhaven, FRG). Quoted are Leg and Site number, position, number of samples, water depth and age of the samples.

Leg	Site	Position	Region	n	Depth/ mbsf	Age/Ma
26	253	24°53′S 87°22′E	Ninetyeast-Ridge	10	1962	4 to 39
42	374	35°51′N 18°12′E	Messina-Plain	4	4088	2 to 5
40	363	19°39′S 9°3′E	Walfish-Ridge	6	2248	50 to 55
80	548	48°55′N 12°10′W	Goban Spur	2	1251	54 to 56
119	738	62°43′S 82°47′E	Kerguelen-Plateau	15	2307	37 to 81
119	744	61°35′S 80°36′E	Kerguelen-Plateau	6	2253	0.5 to 40
121	752	30°54′S 93°35′E	Broken-Ridge	2	1097	23 to 30
122	762	19°53′S 112°15′E	Exmouth-Plateau	9	1371	39 to 50

4. RESULTS

Lithium contents, δ^6Li-values, trace element contents, and carbon and oxygen isotope ratios are given in Table 3. Marine biogene carbonates contain 0.2 to 4 ppm Li, their δ^6Li-values vary by more than 50‰ from −9‰ to +43‰. Only 10% of the carbonates have lithium isotope signatures above +30‰ or below −5‰. Thus, the majority of samples varies within a range of ±35‰.

The mean lithium concentration of recent bivalvia shells is 2.8 ppm. δ^6Li shows a relative narrow variation between +10‰ and +17‰ (Ø = +13‰). This means that the lithium isotope composition of litoral bivalvia is distinctively lighter than ocean water.

4.1. Foraminifera

Holocene foraminifera from Walfish-Ridge show a lithium content of 2.7 ppm on average. Their mean lithium isotope composition is +16‰, which is similar to the value obtained for recent bivalvia shells. One sample with a δ^6Li-value of +25‰ is extremely light. Pliocene foraminifera from the Indian Ocean and the Mediterranean Sea with +17 to +23‰ possess a slightly lighter isotope composition, except one sample with +13‰.

Foraminifera up to an age of 57 Ma (Fig. 3) vary within a large range of 38‰ (between −9‰ and +29‰). A variation in the same order of magnitude has been reported recently for four Pleistocene foraminifera samples by You and Chan (1996). An especially heavy isotope signature has been found in the Middle Eocene at 45 Ma. Low δ^6Li-values occur as well in the Upper Miocene at 11 Ma, in the Oligocene at 32 Ma, and in the Upper Paleocene at 57 Ma. Light lithium isotope compositions are observed in the Lower Miocene at 19 Ma, the Upper Eocene at 39 Ma, and near the Eozcene-Paleocene-boundary at 52 Ma. For better visualisation and for compensation of analytical errors a smoothed curve has been calculated. Smoothing was done by the method of "distance weighted least squares." The resulting curve is characterised by four minima and four maxima. The periodicity, i.e., the distance between two max-

ima or minima following each other, is in the order of 15 Ma.

4.2. Carbonate Ooze

With a total range of 37‰ (+6‰ to +43‰) in δ^6Li, carbonate oozes are characterized by variations similar to foraminifera, except that the means are shifted about 15‰ towards lighter isotope signatures. Possible reasons for this shift might be due to diagenetic effects or an admixture of lithium from the shale fraction during dissolution of the samples. As shown by Chan et al. (1994), the clay-minerals of You et al. (1995) often show relatively light isotope composition which is in accordance with our own data of hemipelagic sediments from the Sea of Japan (Fig. 5). Therefore, δ^6Li values derived from bulk carbonate sediments should be regarded with caution and will be excluded when discussing changes in the paleo-ocean chemistry.

Especially low δ^6Li can be found between 41 and 57 Ma and for samples older than 76 Ma. The Eocene/Oligocene-Boundary (40 Ma) is marked by very light isotope signatures as well as the Cretaceous/Tertiary-Boundary (65 Ma). Smoothing reduces the mean variation of the dataset to 25‰.

4.3. Phanerozoic Limestones

Phanerozoic limestones contain 0.4 to 2.7 ppm lithium (Ø = 1 ppm). This is in contradiction to previously published data which give 5 ppm as mean lithium concentration of limestones (e.g., Heier and Billings, 1970; Ohrdorf, 1968). These earlier data rely on bulk rock analyses, in which lithium from clay-mineral impurities, oxides, or organic matter is incorporated. The trace element contents analysed in this study represent the lithium content of the carbonates only.

The δ^6Li of Phanerozoic limestones varies between +12‰ and +34‰ (Ø = +22‰). For the Cenomane limestone, replicate analyses yield a mean of +34‰, whereas the mixture of Cretaceous limestones has a lower δ^6Li of +25‰. The heaviest lithium isotope compositions have been found for Jurassic limestones: The "Korallenoolith" (Malm) has a δ^6Li of +17‰, and the mixture of Jurassic limestones show a value of +12‰. A secondary vein calcite from the "Korallenoolith" locality is −0.6‰, distinctively heavier than the surrounding limestone. Triassic limestones are very close to each other and have a mean δ^6Li of +22‰. The mixture of Devonian limestones with +31‰ is again very light.

5. DISCUSSION

In order to understand the possible causes of the variations in lithium isotope composition observed in foraminifera, carbonate oozes and limestones, the following processes have to be taken into consideration:

1) vital effects
2) temperature dependent lithium isotope fractionations
3) sample contaminations
4) diagenesis
5) lithium isotope variations of the paleo-ocean

5.1. Vital Effects

The more or less constant offset in δ^6Li of +13‰ of recent marine bivalvia and Holocene foraminifera relative to modern ocean water may be regarded as evidence for a kinetic metabolic fractionation of lithium isotopes during biogene carbonate precipitation ("vital-effect"). Nevertheless, we do not argue that vital effects are the major cause for the observed large variations in lithium isotope composition. Planktonic foraminifera exclusively belong to the class of *globigerinidae* and *globorotaliidae*. Within these closely related families large differences in lithium isotope composition in the order of 15‰ are very unlikely. Instead only small vital effects should be expected if there are any at all.

5.2. Temperature-Dependent Fractionations

The only evidence for a temperature dependence of the lithium concentration has been provided for brachiopode shells (Delaney et al., 1989). Delaney (1986) found no correlation between lithium content in foraminifera and ambient water temperature. Whether or not the isotope signature will be effected by such a process is still unknown. Nevertheless, it appears very unlikely that the small differences in the temperature of ocean waters might be responsible for the large lithium isotope variations observed in foraminifera.

5.3. Sample Contamination

A lithium contamination of the samples by small amounts of clay minerals, organic material, and/or coatings of oxide minerals and baryte might be a potential source of error. Aggressive sample treatment with complexing and reducing agents to remove these impurities, as practised by Boyle (1981) and Lea and Boyle (1991), was not applied; instead specific trace elements were used as contamination indicators: Literature data for Al, K, Rb, Sr, and Mn given by Bender et al. (1975), Boyle (1983), Delaney et al. (1985), Denison et al. (1994), Milliman (1974), and Puechmaille (1994) as mean values for foraminifera were taken as primary element contents. Concentrations distinctly deviating from these values were considered to indicate sample impurities. Correlation of δ^6Li or lithium concentration with Mn gives further evidence for lithium contamination from Mn oxide coatings. Likewise, correlations of Al, K, and Rb with Li or δ^6Li point to the admixture of clay-mineral-lithium. Following this approach thirteen samples have been removed from the database and are not considered in the following discussion.

5.4. Carbonate Diagenesis

During compaction and consolidation of carbonate sediments a recrystallisation of the original biogene carbonate structure may occur. This alteration generally takes place in equilibrium with ocean water and pore fluids, respectively. As is well known Sr and Na may already be influenced during early stages of carbonate diagenesis (e.g., Morse and Mackenzie, 1990). Thus, in order to minimize the risk of alterations due to diagenetic overprint, only morphologically well-preserved foraminifera shells were chosen for analysis.

Table 3. Isotope and trace element data of foraminifera, carbonate oozes, limestones and recent bivalvia.

Sample	Site	Depth m	Age Ma	δ^6Li ‰	s	δ^{18}O ‰	δ^{13}C ‰	Li ppm	Na ppm	K ppm	Rb ppm	Mg ppm	Sr ppm	B ppm	Al ppm	Mn ppm
Foraminifera																
F3-5-129	253	26.3	4.2	20.0	3.3	1.49	1.36	1.4	830	46	4.2	805	805	6.5	221	72
F5-4-116	253	43.2	10.0	−2.2	1.2	1.85	1.54	1.5	776	42	3.9	732	730	6.5	40	75
F7-5-121	253	64.2	13.0	2.2	3.7	1.96	1.45	1.4	952	56	4.2	878	745	6.2	63	93
F8-3-116	253	70.7	14.0	12.4	2.0	1.57	1.81	1.6	634	44	4.6	781	780	5.4	56	107
F9-6-116	253	84.7	21.0	13.9	3.7	1.58	1.14	1.3	657	62	4.3	745	794	6.1	51	100
F10-2-116	253	88.2	27.0	−3.1	2.9	1.38	0.41	1.3	720	76	3.8	1000	770	7.6	57	90
F13-5-31	253	120.3	37.0	−1.5	3.3	1.07	1.47	1.3	647	54	3.8	1000	600	4.9	86	178
F16-1b	253	143.3	38.5	8.3	2.1	0.82	1.48	1.3			3.6			6.6	207	90
F16-4-143	253	148.4	39.5	28.7	2.0	0.51	1.83	1.5	537	305	3.3	800	580	5.4	357	137
F1-75	363	278.0	48.5	−0.4	1.3	−0.37	0.82	0.5	361	65	0.7	1038	556	2.7	240	315
F2-75	363	279.5	49.5	14.9	1.7	0.06	1.34	0.6	291	55	0.5	963	478	3.1	150	418
F3-75	363	281.0	50.5	12.5	1.6	−0.02	1.39	1.0	293	103	0.8	1044	531	4.1	95	275
F4-75	363	282.5	51.5	10.6	2.6	0.15	1.58	0.7	342	88	0.8	800	515	3.1	179	238
F5-75	363	284.0	52.5	5.8	2.1	0.00	1.78	0.7	400	193	0.8	813	588	3.4	135	226
F6-77	363	285.5	53.5	17.1	1.3	0.04	1.44	0.5	484	297	1.1	925	688	2.8	130	306
F-CC	363	286.2	55.0	−5.2	2.3	−0.10	1.43	0.6	350	50	0.4	856	586	2.9	151	296
F5-2-24	374	39.7	2.0	22.8	3.2	0.76	−0.84	1.8	1250	174	4.2	1300	950	10.9	123	64
F6-5-10	374	53.6	3.0	12.9	2.0	0.76	−1.19	2.2	1260	106		1220	940	17.8	192	62
F7-4-26	374	61.8	3.5	23.1	1.9	1.03	0.59	1.4	1050	134	5.0	1570	840	9.6	57	68
F10-1-123	374	86.7	4.5	16.8	1.5	1.14	−0.36	1.6	1050	142	4.8	940	755	3.0	127	43
F4-33	548	247.8	54.5	10.5	2.9	−0.96	0.75	0.7	522	163	1.4	913	713	5.1	239	142
F5-15	548	249.2	56.5	−1.9	0.8	−1.21	0.97	1.4	510	320	3.3	1350	760	9.3	326	116
F1-65	752	90.7	23.3	11.3	1.8	0.61	1.43	0.9	703	70	1.5	1269	731	7.9	198	98
F5-99	752	97.0	29.4	1.9	2.3	1.18	1.61	0.5	286	172	0.5	275	356	2.9	235	79
F4-4-135	762	194.9	39.0	14.3	3.4	0.11	0.51	1.4	749	163	3.3	710	545	5.6	256	120
F8-5-38	762	233.4	41.0	−3.0	2.5	−0.08	0.45	1.0	452	577	1.8	366	796	3.1	134	175
F9-1-48	762	237.0	41.5	−4.1	2.8	0.04	1.09	0.9	562	334	1.4	811	936	7.1	96	187
F11-2-116	762	258.2	43.5	−7.9	1.8	0.38	1.76	0.7	524	312	1.4	549	905	4.3	179	217
F11-6-110	762	264.1	44.0	1.8	1.8	0.35	1.54	0.3	581	567	1.1	700	775	4.2	87	202
1F2-6-71	762	273.2	45.0	−9.4	3.1	0.49	1.17	0.5	552	768	1.3	738	858	3.9	157	177
F16-1-43	762	303.4	46.0	−0.1	3.8	0.16	1.47	0.2	561	548	0.8	586	835	1.9	54	93
F18-2-70	762	324.2	47.0	0.0	5.8	−0.29	1.52	0.6	540	800	1.3	925	688	2.7	146	197
F1100-4	Meteor 9	0.00	0.02	17.8	3.3	0.32	0.00	2.5	1250	214	2.9	1860	910	22.8	57	203
F1	RV-PS2110-1	0.01	0.002	13.1	2.0	0.70	0.20	1.8	1305	154	5.6	683	952	10.7	264	243
F3	RV-PS2110-1	0.03	0.004	11.3	3.4	0.54	0.02	1.9	1366	122	5.5	680	976	10.6	243	203
F5	RV-PS2110-1	0.05	0.006	24.9	2.1	0.76	0.34	2.0	1293	110	5.7	670	927	14.2	257	108
F8	RV-PS2110-1	0.08	0.008	14.5	2.6	0.53	0.39	2.6	1300	127	6.4	659	964	10.0	260	66
F11	RV-PS2110-1	0.11	0.010	15.2	3.3	0.70	−0.13	2.2	1366	112	5.8	670	965	15.9	229	57
Mean				8.4	2.5	0.53	0.94	1.2	738	209	2.9	882	752	6.9	161	156

Table 3. (Continued)

Sample	Site	Depth m	Age Ma	δ^6Li ‰	s	δ^{18}O ‰	δ^{13}C ‰	Li ppm	Na ppm	K ppm	Rb ppm	Mg ppm	Sr ppm	B ppm	Al ppm	Mn ppm
Carbonaceous Oozes																
N4H2-46	744	25.2	9.0	24.6	2.2	3.08	1.20	0.9	322	277	0.90	606	1281	2.4	502	78
N6H3-46	744	45.7	10.8	21.1	3.2	3.68	2.76	0.2	226	131	0.43	563	1525	2.0	165	42
N12H6-46	744	106.9	27.2	22.9	2.5	1.96	1.85	3.0	339	341	2.57	656	1163	3.4	743	92
N14H6-46	744	126.2	33.1	30.6	3.3	2.06	1.60	2.2	318	325	1.14	728	956	2.1	590	105
N18H6-46	744	155.4	37.2	23.2	3.9	1.29	2.40	2.5	228		0.67	563	1488	1.5	179	141
N6H1-48	738	42.5	39.0	39.2	2.1	1.44	2.17	3.3	232	184	0.5	563	1275	1.4	166	109
N20H7-46	744	175.7	39.8	34.1	1.7	0.46	1.90	2.3	269	273	0.59	388	1313	1.2	86	200
N7H5-48	738	57.8	40.1	29.8	1.8	1.30	1.77	2.3	233	178	0.5	763	1250	1.4	137	116
N9H3-48	738	74.0	41.5	42.8	2.4	1.05	2.01	1.2	224	240	0.6	464	1225	1.5	66	86
N12H5-48	738	101.0	42.5	17.8	1.1	0.62	2.22	2.3	245	291	0.8	425	1375	1.4	118	112
N15X5-48	738	124.3	44.9	8.1	3.3	0.60	1.67	1.2	250	297	0.7	575	1315	2.4	67	146
N18X3-48	738	150.3	46.4	11.5	2.6	−0.09	1.63	2.7	150	43	0.3	681	1100	1.8	73	99
N22X3-48	738	188.9	47.9	40.0	1.1	0.21	1.20	1.8	228	81	0.6	620	1313	1.0	82	123
N5R1-46	738	226.1	52.5	11.1	2.2	−0.41	0.89	0.6	213	144	0.8	800	1075	2.8	63	141
N10R2-36	738	275.7	55.7	7.3	2.7	−0.62	1.12	0.7	450	96	1.9	519	856	2.3	70	190
N20R2-50	738	372.2	64.6	30.6	2.9	−0.84	2.45	0.8	250	338	1.9	913	719	2.2	233	339
N23R2-47	738	401.2	67.5	31.7	2.1	−0.61	1.62	1.0	378	244	0.9	738	950	3.5	137	170
N25R1-64	738	419.2	71.2	30.5	1.9	−1.07	2.42	2.3	226	238	1.8	434	1306	1.9	122	132
N27R3-49	738	441.4	75.4	20.0	2.4	−1.34	2.26	0.4	219	193	1.5	785	725	1.9	130	347
N29R2-48	738	459.2	79.0	6.2	2.8	−2.43	2.58	0.6	349	313	1.4	763	481	2.5	186	402
N30R2-48	738	468.6	80.9	12.6	2.3	−1.91	2.34	0.5	709	163	1.7	688	419	1.7	230	548
Mean				23.6	2.4	0.40	1.91	1.6	288	220	1.1	630	1100	2.0	197	177
German Limestones																
Cenoman	Söhlde			33.5	3.6	−1.72	2.72	1.7	290	194	2.72	1433	563	5.53	615	567
Cretaceous-mix				25.1	2.7	−3.62	0.67	2.7	256	1081	5.65	2419	681	5.5	1520	589
Koralenoolith	Salz-Hemmendorf			17.4	2.5	−2.33	2.25	0.6	266	214	2.06	6063	205	1.3	148	108
Koralenoolith (vein)	Salz-Hemmendorf			−0.6	3.0	−6.16	0.32	0.2	31	20	0.17	1563	43	1.6	32	113
Jura-mix				11.7	0.3	−3.75	−0.90	1.5	193	370	1.84	3934	234	2.8	858	834
Trias mo1	Hünenburg			25.2	3.8	−4.85	2.20	0.6	105	386	1.66	2781	556	2.8	1068	238
Trias mu2	Dransfeld			23.3	5.6	−3.23	0.20	1.1	175	103	0.66	6375	433	2.8	137	303
Trias mu1	Reckershausen			27.1	2.1	−6.81	0.18	0.4	174	43	0.36	2438	244	1.0	89	298
Devonian-mix				31.4	1.1	−8.10	1.07	1.0	103	500	2.55	6031	244	0.7	523	828
Mean				21.6	2.7	−4.51	0.97	1.1	177	323	1.96	3671	356	2.7	554	431
Bivalvia																
Abra	Nordsee			16.5	2.8	1.05	−0.41	2.5	6400	37	7.2	98	1200	5.6	4.5	17
Barnea	Nordsee			10.2	3.0	0.46	−0.26	1.3	6200	56	5.2	122	1150	4.4		18
Cardium	Nordsee			12.7	2.2	0.30	−0.04	3.8	3350	41	4.6	136	1620	11	12	19
Ensis	Nordsee			14.6	1.4	1.51	−1.14	4.0	5500	36	5.9	124	1250	3.8	3.6	9
Macoma	Nordsee			15.1	2.5	0.91	−0.22	1.9	5400	40	7.8	105	1700	2.8	6.4	21
Mya	Nordsee			11.2	2.0	0.64	0.38	3.8	5100	52	7.5	130	1450	3.9	3.5	19
Mytilus	Nordsee			11.3	2.0	0.68	−0.68	2.6	3700	23	4.4	870	860	9.6	3.6	70
Mean				14.8	2.5	0.8	−0.34	2.8	5093	40.7	6.1	226.4	1319	5.9	5.7	25

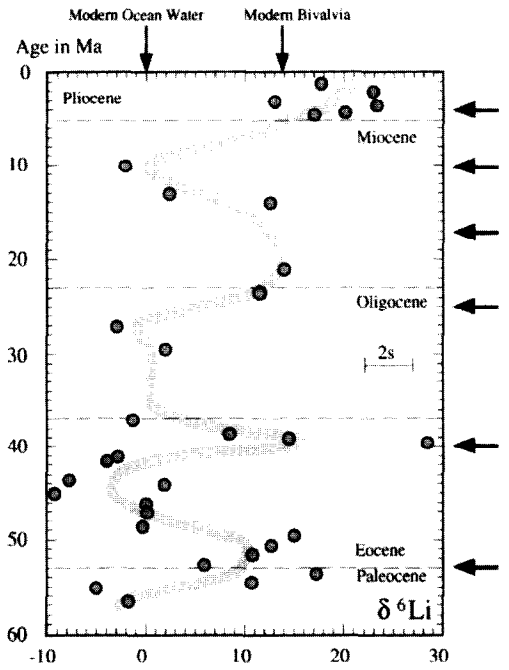

Fig. 3. δ^6Li of foraminifera up to an age of 57 Ma (Sites 253, 363, 548, 752, and 762). The curve was smoothed with DWLS ("distance weighted least squares"). On the right axis phases of global plate reorganisations and mountain-building, in connection with increased MOR-spreading activity, are marked with arrows (Rampino and Caldeira, 1993).

In cases where signs of alteration were revealed during visual inspection of the formaminifera under the stereomicroscope, the sample was discarded. In order to get better control of the degree of alteration, Na, Mg, Sr, B, and Mn contents as well as oxygen and carbon isotope compositions of the samples were determined (Fig. 4). The foraminifera samples analysed in this study have a mean lithium concentration of 1.2 ppm (range: 0.5 to 2.6 ppm) which is close to 0.9 ppm given by Delaney (1986). Delaney (1986) subjected her samples to a radical cleaning procedure and we interpret the slightly lower lithium concentrations reported by Delaney (1986) as being due to a loss of loosely bound lithium from the upper layers of the carbonates during the action of complexing chemicals. We take the general agreement between both datasets as evidence that the original lithium concentration and lithium isotope signature of foraminifera has not been completely overprinted by diagenesis.

Lithium, Na, Rb, Sr, B contents, and δ^{18}O of foraminifera are decreasing during the Tertiary, whereas Mn concentrations are increasing (see Fig. 5). δ^6Li is positively correlated with Li (r = 0.52), Na, and B, which might be interpreted as evidence for a diagenetic control of the lithium isotope composition. However, there is no correlation between δ^6Li and δ^{18}O.

More pronounced correlations are observed, however, among Li, Sr, and Mn in the carbonate oozes. Additionally, there is a positive correlation between δ^6Li and δ^{18}O and a negative one with B, which could not be found in the foraminifera data. Obviously carbonate oozes are more affected by diagenesis than foraminifera. This seems to be due to the fine-grained nature of carbonate particles being more sensitive to alteration. The Phanerozoic limestones, which have been selected to obtain more detailed information about how lithium contents and lithium isotope ratios might be altered during diagenesis show no trend, which can be related to age-dependent diagenetic reactions.

In summary there are some evidences available that foraminifera retain their primary δ^6Li signal. We, therefore, tentatively conclude that the lithium isotope signatures are not seriously affected by diagenetic alteration, even if partial loss of lithium occured. δ^6Li-values of bulk carbonates, however, should be interpreted with caution, because they are more dependent on intense recrystallisation and exchange reactions with porewaters. Eventually, this may cause a shift in the lithium isotope signal.

5.5. Variations in Paleo-Ocean Chemistry

We first consider the lithium isotope composition of important geological reservoirs based on our own analyses and data from Chan and Edmond (1988), Chan et al. (1992, 1993, 1994), You and Chan (1996), and You et al. (1995) (see Fig. 5). Fresh oceanic basalts have a mean δ^6Li of 32‰ (Chan et al., 1992, 1993; K. Mengel, unpubl. data). For submarine hydrothermal-solutions a δ^6Li between +24‰ and +33‰ (Ø = 27‰) has been reported from the East-Pacific Rise, the Mid-Atlantic Ridge, and from the Guaymas-Basin (Chan et al., 1993, 1994). The slightly heavier isotope composition in some samples may be caused by retrograde reactions with increasing water/rock ratios and decreasing temperatures near the vents. Spilitised basalts have a mean δ^6Li of +19‰ relative to ocean water (Chan et al., 1992, 1993; K. Mengel, unpubl. data). Assuming that MORBs lose 50% of their primary lithium content during HT-alteration and that the residual lithium retains its original isotope signature, the fractionation factor effective during spilitisation (α'_{LT}) can be estimated as 1.013 which is somewhat smaller compared to the fractionation factor of 1.019 given by Chan and Edmond (1988). δ^6Li of freshwater in rivers and lakes varies between +4 and +18‰ (Chan et al., 1992; own unpublished results). For the following considerations a global mean value of +9‰ was assumed. For hemipelagic marine sediments from the Nankai-Basin and the Guaymas Basin (DSDP Site 477), Chan et al. (1994) and You et al. (1995) observed δ^6Li values between +28‰ and +38‰ (Ø = +30‰). Taking this value together with own unpublished results for hemipelagic sediments from the Sea of Japan (ODP Leg 127) we adopt a mean value of +28‰ for marine sediments.

Assuming that the lithium isotope signature of the continental crust is similar to the δ^6Li of the mantle (+32‰) and taking a δ^6Li of the river input of +9‰ into account, it is possible to estimate the lithium isotope ratio of river particulate matter (=RPM). According to Chester (1990), the annual lithium flux in the form of RPM should be about four times higher than the dissolved lithium flux. Then a δ^6Li value of 38‰ for RPM can be estimated. Such a light value can be expected due to ion-exchange-reactions during weathering, where ^{6}Li is preferentially enriched in the weathering residuum. Figure 6 summarizes the mean lithium iso-

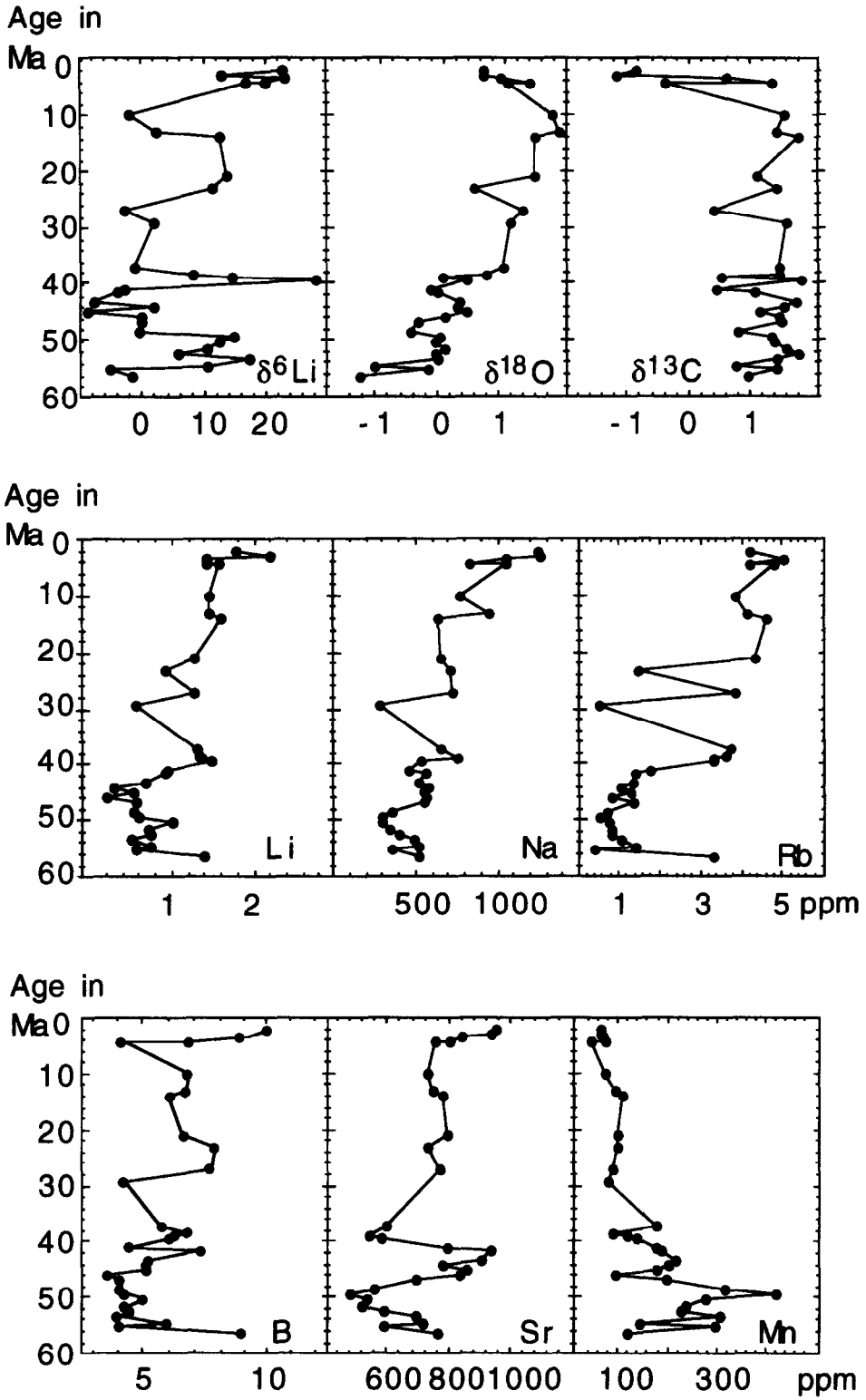

Fig. 4. Isotope and trace element profiles of Quaternary and Tertiary foraminifera samples.

tope composition of the sources and sinks in the global lithium isotope cycle and gives an estimate of the respective fractionation factors.

Our investigations showed that foraminifera will preserve their original lithium isotope signature after deposition. This conclusion implies that fossil foraminifera represent the lithium isotope composition of the ocean water at the time of their formation. Table 4 summarizes the geological processes

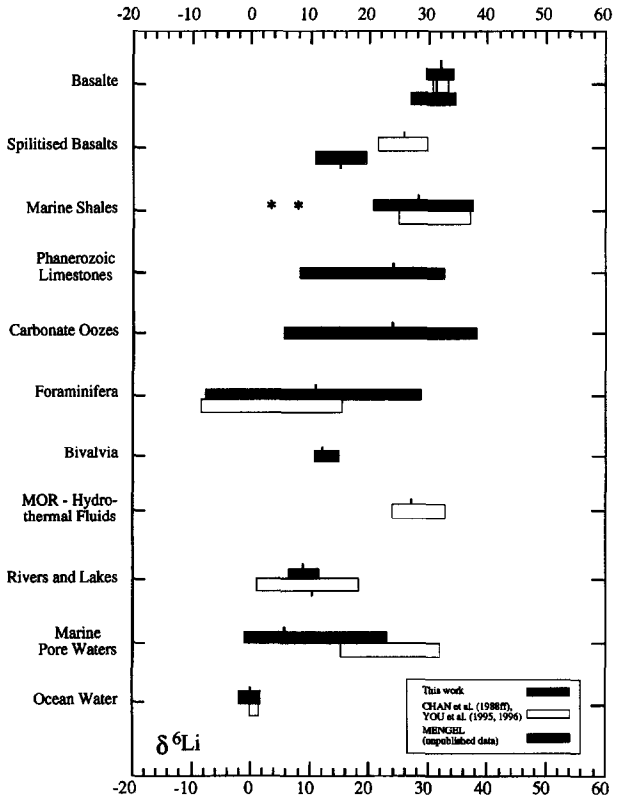

Fig. 5. Range of natural lithium isotope compositions in igneous rocks, sediments, MOR-hydrothermal fluids, and freshwater based on our own analyses and data from Chan et al. (1988, 1992, 1993, 1994) and You et al. (1995). Single outliers are marked by "*".

having a characteristic imprint on the lithium isotope composition of ocean water. High temperature ocean water/basalt interactions cause a decrease in the lithium content of basalts and an increase in the lithium concentration of the ocean. Lithium liberated during this high-temperature process and

Table 4. Processes which affect the Li-isotope composition of ocean water (+ means an increase in δ^6Li, − means a decrease in δ^6Li).

Geological process	δ^6Li (ocean)
hydrothermal alter. (HT)	++
continental weathering	+
hydrothermal alter. (LT)	−
authigenic clay formation	−−

supplied to the ocean should have an isotopic composition similar to that of the basalts. On the other hand, river water with a mean isotope composition of 9.0‰ (see Fig. 5) has a considerably smaller effect on the lithium isotope composition of ocean water than the high temperature flux.

These two processes thus supply the ocean with lithium being enriched in ^{6}Li. As required by a steady-state ocean, appropriate sink reactions must provide a mechanism for the preferential removal of the light lithium isotope. Although until today very few data are available about lithium isotopic compositions in shales and soils, there is strong evidence for a fractionation of lithium isotopes during weathering and clay mineral diagenesis. According to early experiments by Taylor and Urey (1938) and estimates based on model considerations, fractionation processes must be in the order of 20‰ with a preferential enrichment of ^{6}Li in the solid phase. Thus, the most efficient process to remove ^{6}Li from the ocean is authigenic clay mineral formation followed by low-temperature alteration processes of the oceanic crust.

Finally, we will examine the question whether or not variations in the rates of these four flux reactions in the geologic past might be able to balance the observed lithium isotope variations of about 15‰. There is abundant evidence that hydrothermal activity at the ridges and erosion rates have varied considerably during the Earth's history, whereas there is little evidence that rates of clay mineral formation and low-temperature ocean crust alteration varied throughout time.

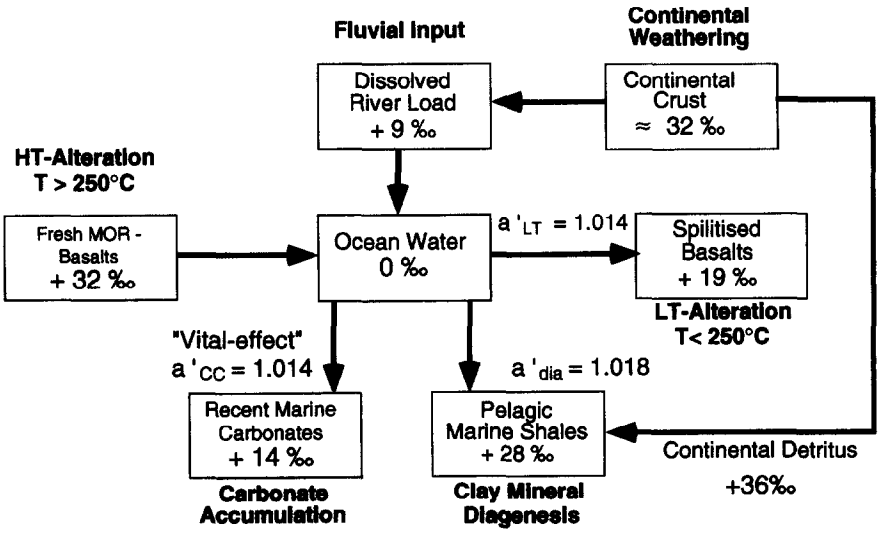

Fig. 6. Lithium isotope balance of ocean water and estimated lithium isotope fractionation factors.

Therefore, we consider variations in the two lithium sources only to be responsible for changes in the lithium budget.

An increase of the riverine lithium flux should lead to a decrease in ocean water δ^6Li and the reverse effect will be observed when the fluvial lithium input becomes smaller. An increase of the HT-lithium flux may lead to an increase in ocean water δ^6Li. Thus, in a steady-state ocean, HT input rates and fluvial input rates behave antagonistic, i.e., high HT input rates in conjunction with low fluvial fluxes induce the largest shifts in the lithium isotope ratios of ocean water. In contrast, simultaneous decreases in HT flux rates and increases in fluvial-flux rates or vice versa possibly may compensate each other leaving ocean water δ^6Li unaffected.

In this connection we have also to consider the consequences of these reactions for the lithium concentration of ocean water. As has been argued by Holland (1984), Delaney (1986), and Delaney et al. (1989) a shift in lithium concentration during the Phanerozoic exceeding the factor of 2 can be regarded as unlikely. Given a lithium concentration of 175 ppb for modern ocean water this would correspond to 90 ppb for the lower limit and 350 ppb for the upper limit for a non-steady-state ocean, being equivalent to a variation in the HT inputs and fluviatile inputs between +100% and −50%. Such changes in the two lithium sources lead to shifts of 15‰ in δ^6Li.

If the changes in lithium isotope ratios observed in planktonic foraminifera are induced by variations in the global ocean water composition, then correlations can be predicted between the lithium isotope curve, production rates of oceanic crust, phases of global plate reorganisations, and periods of intense mountain-building. From these parameters, phases of enhanced submarine hydrothermal activity associated with tectonic seafloor rearrangements at 2, 17, 25, 40, and 53 Ma (Rampino and Caldeira, 1993) indeed coincide with high δ^6Li-values in foraminifera. We also compared our lithium isotope curve with published δ^{13}C, δ^{18}O, δ^{34}S, or ^{87}Sr/^{86}Sr seawater curves, but there seems to be no further correspondence. Future investigations have, of course, to verify these preliminary conclusions.

Acknowledgments—H.-J. Brumsack, W. U. Ehrmann, A. Mackensen, N. Scheele, and H. Oberhänsli provided sample material and important geological and paleontological background information, which is gratefully acknowledged. We thank K. Mengel, K. Simon, and M. Pohlmann for helpful discussions. Tom Bullen, Marc Chaussidon, Toni Eisenhauer, and an anonymous reviewer provided constructive reviews, which helped us to clarify our views. This research was financially supported by the "Deutsche Forschungsgemeinschaft" (DFG) within the "Schwerpunktprogramm" of Ocean-Drilling-Project (ODP).

Editorial handling: G. Faure

REFERENCES

Bender M. L., Lorens R. B., and Williams D. F. (1975) Sodium, magnesium and strontium in the tests of planktonic foraminifera. *Micropalaeontology* **21,** 448–459.

Boerboom A. J. H. (1989) Isotope effects in thermal ionization of LiCl. *Intl. J. Mass Spec. Ion Proc.* **93,** 303–307.

Boyle E. A. (1981) Cadmium, zinc, copper and barium in foraminifera tests. *Earth Planet. Sci. Lett.* **53,** 11–35.

Boyle E. A. (1983) Manganese carbonate overgrowth on foraminifera tests. *Geochim. Cosmochim. Acta* **47,** 1815–1819.

Broecker W. S. (1974) *Chemical Oceanography.* Harcourt Brace Jovanovich.

Brown H. L., Biltz C., and Anbar M. (1977) A precision isotope ratio mass spectrometer for the analysis of ^{6}Li/^{7}Li. *Intl. J. Mass Spectrom. Ion Phys.* **25,** 167–181.

Calvert S. E. (1974) Deposition and diagenesis of silica in marine sediments. In *Pelagic Sediments* (ed. K. J. Hsü and H. C. Jenkins); *Intl. Assoc. Sediment. Spec. Publ.* **1,** 273–299.

Chan L. H. (1987) Lithium isotope analysis by thermal ionization mass spectrometry of lithium tetraborate. *Anal. Chem.* **59,** 2662–2665.

Chan L. H. and Edmond J. M. (1988) Variation of lithium isotope composition in the marine environment: A preliminary report. *Geochim. Cosmochim. Acta* **52,** 1711–1717.

Chan L. H., Edmond J. M., Thompson G., and Gillis K. (1992) Lithium isotopic composition of submarine basalts: implications for the lithium cycle in the oceans. *Earth Planet. Sci. Lett.* **108,** 151–160.

Chan L. H., Edmond J. M., and Thompson G. (1993) A lithium isotope study of hot springs and metabasalts from midocean ridge hydrothermal systems. *J. Geophys. Res.* **98 B6,** 9653–9659.

Chan L. H., Gieskes J. M., You C. F., and Edmond J. M. (1994) Lithium isotope geochemistry of sediments and hydrothermal fluids of the Guaymas Basin, Gulf of California. *Geochim. Cosmochim. Acta* **94,** 4443–4454.

Chester R. (1990) *Marine Geochemistry.* Unwin Hyman.

Datta B. P., Khodade P. S., Parab A. R., Goyal A. H., Chitambar S. A., and Jain H. C. (1992) Thermal ionization mass spectrometry of Li_2BO^{2+} ions: Determination of isotopic abundance ratio of lithium. *Intl. J. of Mass Spectrom. Ion Proc.* **116,** 87–114.

Delaney M. L. (1986) Lithium in foraminiferal shells: implications for high-temperature hydrothermal circulation fluxes and oceanic crustal generation rates. *Earth Planet. Sci. Lett.* **80,** 91–105.

Delaney M. L., Bé A. W. H., and Boyle E. A. (1985) Li, Sr, Mg and Na in foraminiferal calcite shells from laboratory culture, sediment traps and sediment cores. *Geochim. Cosmochim. Acta* **49,** 1327–1341.

Delaney M. L., Popp B. N., Lepzelter C. G., and Anderson T. F. (1989) Lithium-to-calcium ratios in modern Cenozoic and Paleozoic articulate brachiopod shells. *Paleoceanography* **4,** 681–691.

Denison R. E., Koepnick R. B., Fletcher A., Howell M. W., and Callaway W. S. (1994) Criteria for the retention of original seawater ^{87}Sr/^{86}Sr in ancient shelf limestones. *Chem. Geol.* (Isotope Geosciences Section) **112,** 131–143.

Edmond J. M., Measures C., McDuff R. E., Chan L. H., Collier R., Grant B., Gordon L. I., and Corliss J. B. (1979) Ridge crest hydrothermal activity and the balance of the major and minor elements in the ocean: The Galapagos data. *Earth Planet. Sci. Lett.* **46,** 1–18.

Flesch G. D. and Svec H. J. (1973) A secondary isotopic standard for ^{6}Li/^{7}Li determinations. *Intl. J. Mass. Spec. Ion. Phys.* **12,** 265–272.

Garrels R. and Mackenzie R. M. (1971) *Evolution of Sedimentary Rocks.* W. W. Norton.

Green L. W., Leppinen J. J., and Elliot N. L. (1988) Isotopic analysis of lithium as thermal dilithium fluoride ions. *Anal. Chem.* **60,** 34–37.

Habfast K. (1983) Fractionation in the thermal ionization source. *Intl. J. Spectrom. Ion Phys.* **51,** 165–189.

Harland W. B., Armstrong R. L., Cox A. V., Craig L. E., Smith A. G., and Smith D. G. (1989) *A Geologic Time Scale,* rev. ed. Cambridge University Press.

Heier K. S. and Billings G. K. (1970) Lithium. In *Handbook of Geochemistry* (ed. K. H. Wedepohl). Springer-Verlag.

Holland H. D. (1984) *The Chemical Evolution of the Atmosphere and Oceans.* Princeton University Press.

Ishikawa T. and Nakamura E. (1993) Boron isotope systematics of marine sediments. *Earth Planet. Sci. Lett.* **117,** 567–580.

Lea D. W. and Boyle E. A. (1991) Barium in planktonic foraminifera. *Geochim. Cosmochim. Acta* **55,** 3321–3331.

Maxwell J. A. (1963) Geochemical study of some chert and related deposits. *Bull. Geol. Surv. Canada* **104,** 1–31.

McCrea J. M. (1950) The isotope chemistry of carbonates and a paleotemperature scale. *J. Chem. Phys.* **18,** 849–857.

Mengel K. and Hoefs J. (1990) Li-δ^{18}O-SiO_2 systematics in volcanic rocks and mafic lower crustal granulite xenoliths. *Earth Planet. Sci. Lett.* **101,** 42–53.

Michiels E. and deBiévre P. (1983) Absolute isotopic composition and the atomic weight of a natural sample of lithium. *Intl. J. Mass-Spec. Ion Phys.* **49,** 265–274.

Milliman J. D. (1974) *Marine Carbonates.* Springer-Verlag.

Morse J. W. and Mackenzie F. T. (1990) *Geochemistry of Sedimentary Carbonates. Developments in Sedimentology* **48,** Elsevier.

Ohrdorf R. (1968) Ein Beitrag zur Geochemie des Lithiums in Sedimentgesteinen. *Geochim. Cosmochim. Acta* **32,** 191–208.

Puechmaille C. (1994) Mg, Sr and Na fluctuations in the test of modern and recent Globigerina bulloides. *Chem. Geol.* **116,** 147–152.

Rampino M. R. and Caldeira K. (1993) Major episodes of geologic change: Correlations, time structure and possible causes. *Earth Planet. Sci. Lett.* **114,** 215–227.

Ryan J. G. and Langmuir C. H. (1987) The systematics of lithium abundances in young volcanic rocks. *Geochim. Cosmochim. Acta* **54,** 1727–1741.

Seyfried W. E., Janecky D. R., and Mottl M. J. (1984) Alteration of oceanic crust: Implications for geochemical cycles of lithium and boron. *Geochim. Cosmochim. Acta* **48,** 557–569.

Stoffyn-Egli P. and Mackenzie F. T. (1984) Mass balance of dissolved lithium in the oceans. *Geochim. Cosmochim. Acta* **48,** 859–872.

Stroh A. and Völlkopf U. (1993) Effects of Ca on instrument stability in the trace element determination of Ca-rich soils using ICP-MS. *Atomic Spectroscopy* **14,** 76–79.

Svec H. J. and Anderson A. R., Jr. (1965) The absolute abundance of lithium isotopes in natural sources. *Geochim. Cosmochim. Acta* **29,** 633–641.

Taylor T. I. and Urey H. C. (1938) Fractionation of the lithium and potassium isotopes by chemical exchange with zeolites. *J. Chem. Phys.* **6,** 429–438.

Thompson G. (1983) Hydrothermal fluxes in the ocean. In *Chemical Oceanography,* Vol. 8 (ed. J. P. Riley and R. Chester), pp. 272–338. Academic Press.

von Damm K. L., Edmond J. M., Measures C. I., and Grant B. (1985a) Chemistry of submarine hydrothermal solutions at Guaymas Basin, Gulf of California. *Geochim. Cosmochim. Acta* **49,** 2221–2237.

von Damm K. L., Edmond J. M., Grant B., Measures C. I., Walden B., and Weiss R. F. (1985b) Chemistry of submarine hydrothermal solutions at 21°N, East Pacific Rise. *Geochim. Cosmochim. Acta* **49,** 2197–2220.

Xiao Y. K. and Beary E. S. (1989) High-precision isotopic measurement of lithium by thermal ionization mass spectrometry. *Intl. J. of Mass Spectrom. Ion processes* **94,** 101–114.

You C. F. and Chan L. H. (1996) Precise determination of lithium isotope composition in low concentration natural samples. *Geochim. Cosmochim. Acta* **60,** 909–915.

You C. F., Chan L. H., Spivack A. J., and Gieskes J. M. (1995) Lithium, boron and their isotopes in sediments and pore waters of ODP Site 808, Nankai Trough: Implications for fluid expulsion in accretionary prisms. *Geology* **23,** 37–40.